C.P. No. 236
(17,893)
A.R.C. Technical Report

C.P. No. 236
(17,893)
A.R.C. Technical Report

MINISTRY OF SUPPLY

AERONAUTICAL RESEARCH COUNCIL

CURRENT PAPERS

Investigation of High Length/Beam Ratio Seaplane Hulls with High Beam Loadings Hydrodynamic Stability Part 13 The Effect of Afterbody Angle on Stability and Spray Characteristics

By

D. M. Ridland, A.F.R.Ae.S., G.I.Mech.E.

LONDON HER MAJESTY'S STATIONERY OFFICE

1956

PRICE 4s 6d NET

Report No. F/Res/248
February 1955

MARINE AIRCRAFT EXPERIMENTAL ESTABLISHMENT, FELIXSTOWE, SUFFOLK

INVESTIGATION OF HIGH LENGTH/BEAM RATIO SEAPLANE HULLS WITH HIGH BEAM LOADINGS

HYDRODYNAMIC STABILITY PART 13

THE EFFECT OF AFTERBODY ANGLE ON STABILITY AND SPRAY CHARACTERISTICS

by

D. M. Ridland, A.F.R.Ae.S., G.I.Mech.E

S U M M A R Y

The effects of afterbody angle on longitudinal stability, spray and directional stability characteristics and elevator effectiveness are deduced from the results of tests on three models of the series which were alike in every major respect except that of afterbody angle. The models had afterbody angles of 4°, 6° and 8° respectively.

It was found that increasing afterbody angle improved longitudinal stability characteristics considerably, both with and without disturbance, increased trim generally, gave a slight improvement in spray and directional stability characteristics and increased elevator effectiveness. The best hydrodynamic configuration was that with the 8° afterbody angle.

/ LIST OF CONTENTS

LIST OF CONTENTS

LIST OF TABLES

/ LIST OF FIGURES

LIST OF FIGURES

/ 1. INTRODUCTION

1. INTRODUCTION

In this report the effects of afterbody angle (the angle between the tangents to the forebody and afterbody keels at the main and rear steps respectively) on the hydrodynamic stability and spray characteristics of a high length/beam ratio flying boat are deduced from the results of tests on three models of the series detailed in Reference 1 and listed in Table I. These models, A, G and H, with which this report is concerned, constituted the third phase of the present investigation i.e. the determination of the effects of afterbody angle. They were identical except in respect of afterbody angle and this single parameter was varied in the following manner:

Model G	Afterbody angle 4°
Model A	Afterbody angle 6° (basic model)
Model H	Afterbody angle 8°

The effect of this variation on the hull shape generally can be seen in Figure 1, which is a comparison of hull lines. Hydrodynamic and aerodynamic data common to the three models are given in Tables II and III, but it may be mentioned here that the length/beam ratio of each model was 11 (the forebody was 6 beams in length and the afterbody 5 beams), the forebody was unwarped and the step was of straight transverse type with no fairing and a depth of 0.15 beams. Further details of considerations affecting the design of the models are given in Reference 1.

The same techniques were employed consistently throughout the tests and they are discussed fully, together with the presentation of results, in References 1 and 2. A résumé of the details will be given in relevant sections as the need arises, but several common major factors may, with advantage, be stated here.

All the tests now under consideration were made with zero flap, no slipstream, one C.G. position and, except for the directional stability assessment, at the two beam loadings C_{Δ_0} = 2.75 and 2.25; directional tests were made only at C_{Δ_0} = 2.75. Full details of the tests carried out on each model are given separately in References 3, 11 and 12; only stability limits and sufficient illustrations to indicate the main trends are given here.

Throughout the report conclusions are drawn from comparisons of results at C_{Δ_0} = 2.75 and, where possible, substantiation is obtained from the other weight case. Reference is also made to earlier work on hulls of lower length/beam ratios.

2. LONGITUDINAL STABILITY

2.1. Present tests

Longitudinal stability tests were made by towing the model from the wing tips on the lateral axis through the centre of gravity, with the model free in pitch and heave. The elevator setting was selected before each run and the model towed at constant speed. The angle of trim was noted in the steady condition, and if the model proved stable at the speed selected it was given nose-down disturbances to determine whether instability could be induced, the largest amounts of disturbance being required in the high speed undisturbed lower limit region. In each case the motion was defined as unstable when the resulting oscillation (if any) was apparently divergent or had a constant amplitude of more than 2°. Stability limits were built up by these methods, the disturbed limits representing the worst possible disturbed case. Both undisturbed and disturbed limits for models A, G and H are compared in Figures 2 and 3 for the two weights concerned.

/ The

The effects of afterbody angle on the stability limits for $C_{\Delta_o} = 2.75$ in the undisturbed case are shown in Figure 2(a). With increasing afterbody angle, the available stable trim range is increased throughout the planing range of speeds. The most obvious detailed change is the considerable raising of the upper limit, while the position of the lower limit is almost unchanged at medium and high planing speeds. Maximum lower critical trim (maximum trim attained on the lower limit) is raised about 3° over the range of afterbody angles considered (from 4° to 8°), but the change is not progressive and calls for further comment.

With regard to the effects of afterbody angle on maximum lower critical trim, there is an irregularity in Figure 2(a) which occurs with the afterbody angle of 6° and is due to the formation of a vertical neck of instability across the take-off path; there is thus no true maximum lower critical trim on this set of limits. This leads to consideration of Figure 7 which shows that in the case of the 4° afterbody angle without disturbance, there is a similar neck of porpoising, which extends across the take-off path but is excluded by the limits because the amplitudes are in general less than 2°; in the 8° afterbody angle case there is no corresponding region of porpoising. With increasing afterbody angle, then, the porpoising initially occurring in this region is increased in amplitude to more than 2°, when the motion is formally classed as unstable and there is no true maximum lower critical trim, and then disappears, while the region itself is found at progressively higher attitudes.

Before seeking confirmation of these effects in Figure 3 (a), which is a comparison of undisturbed longitudinal stability limits for the three models at a lower loading, $C_{\Delta_o} = 2.25$, it is necessary to consider the effects of load separately for each model. Examination of References 3, 11 and 12 (or the two figures, 2 (a) and 3 (a)) shows that for a reduction in beam loading, C_{Δ_o}, by 0.5, the lower limits for Models A and G are lowered by similar amounts, about 1.8°, while that for Model H is lowered by about half of this amount. It follows that quantitative substantiation of the afterbody angle effects shown in Figure 2 (a) cannot be obtained directly from Figure 3 (a) and that the difference in the rate of change of critical trim (trim of a point on the stability limit) with respect to load in the case of Model H is one of the results of increasing afterbody angle, i.e. afterbody angle effects on undisturbed stability characteristics are not independent of load.

Considering Figure 3 (a) it will be seen that the main qualitative results are the same as for the higher loading. Increasing afterbody angle results in an increase in the available stable range of trims throughout the planing speed range and the upper limit is raised considerably. The separation of the lower limits is in keeping with the previous paragraph and while there is an ordered increase in maximum lower critical trim, the greater part of this accrues from the first 2° increase in afterbody angle from the lowest value. Although, due to the reduction in weight, there is no post-hump neck of instability, the large increase in maximum lower critical trim obtained with the 6° afterbody angle substantiates the proneness of this model to become unstable in this region.

It is convenient to say here that because of the unexpected separation of the lower limits in Figure 3 (a), the limits for Models G and H at this weight, $C_{\Delta_o} = 2.25$, were checked. Agreement with the original limits was very good, verifying the separation found in Figure 3 (a).

In the disturbed case the effects of afterbody angle variation are shown for the two loadings, $C_{\Delta_o} = 2.75$ and 2.25, in Figures 2 (b) and 3 (b). Before discussing them however, it should be noted that orders rather than absolute amounts of change should be considered because of the experimental limitations in the disturbance technique (References 1, 10).

/ With

With increasing afterbody angle at $C_{\Delta_0} = 2.75$ (Figure 2 (b)), the hump* limit is found at lower speeds and much higher attitudes, while the high speed stable region is increased considerably, with the lower, high speed, extremities of the limits remaining almost coincident. The net result is an over-all improvement in disturbed stability characteristics with increasing afterbody angle with a progressive, but slight, reduction and movement to lower speeds of the speed range over which instability is encountered.

Similar general remarks apply in the lower weight case, Figure 3 (b), but here the progressive improvement in stability with increasing afterbody angle is even more pronounced. The major difference from the higher weight case is found in the high speed lower limit region. Where formerly the limits were coincident, only the lower parts of those for Models A and G now show this tendency (the turn up on Model A limit was obtained only with the most violent disturbances and is not felt to be of immediate significance), while the limit for Model H is raised generally. This effect is similar to that obtained in the undisturbed case, so it may now be said that afterbody angle effects on stability are not independent of load in either undisturbed or disturbed cases.

The effects of afterbody angle on the stability limits are shown in a different light for the two beam loadings, $C_{\Delta_0} = 2.75$ and 2.25, in Figures 4 and 5 respectively, where elevator angles replace keel attitudes as ordinates.

In the undisturbed case (Figures 4 (a) and 5 (a)) it might be expected from previous plots of this nature (References 6 and 10) that the improvement in stability obtained with the higher afterbody angles would not be shown; in general this is the case, but the two features mentioned earlier, viz:

(i) the tendency for the 6° afterbody model to form a post-hump neck of instability, and

(ii) the raising of the lower limit for the 8° afterbody model at the lower loading,

are emphasised. The neck of instability obtained with the 6° afterbody model is clearly shown in Figure 4 (a) and there is an obvious tendency towards the formation of a similar neck at the lower loading in Figure 5 (a). The raising of the limit for Model H is found with this type of presentation not only in the case of the lower limit at the lower loading, but with both limits at both loadings. The lower limits are in order at both weights, those for the lowest afterbody angle being found at the greatest value of elevator setting.

In the disturbed case, at both loadings (Figures 4 (b) and 5 (b)), the movement of the hump limit down the speed scale with increase of afterbody angle is seen to be obtained mainly with the first increment investigated, i.e. from 4° to 6°, while the improvement in the high speed stable region remains progressive. It may be noted that at each weight the high speed, lower limits show a separation and order which corresponds closely to that of the lower limits in the relevant undisturbed case.

/ Apart

---

* Hump limit - The longitudinal stability limit found on the low speed side of a band of instability crossing the take-off path just above hump speed.

Apart from the removal of the neck of instability in the undisturbed case, the main effect of theweight decrease (Figures 4 and 5) is to move the limits bodily down the speed scale, particularly the upper limits. In the disturbed case there is a similar effect, which is accompanied by a slight general increase in the three high speed stable areas.

It should be noted that during the tests just considered the pitching moments of inertia of Models A, G and H were 22.90, 23.50 and 23.50 lb. ft.^{2} respectively at $C_{\Delta_o} = 2.75$ and 24.46, 23.50 and 23.50 lb. ft.^{2} at $C_{\Delta_o} = 2.25$ i.e. all within 7% of the value for Model A. By the conclusions of Reference 2, moment of inertia increases of up to 40% have no appreciable effect on the limits, so the differences in moment of inertia do not affect the foregoing discussions.

Trim curves for $\eta = 0^o$ are given in Figure 6 for all models at the two weights concerned. At $C_{\Delta_o} = 2.75$ (Figure 6 (a)) the effects of increasing afterbody angle are to increase trim progressively from and including the static floating condition, up to speeds just past the hump, when the trim curves tend to run together. It is interesting to note that the increase in hump trim is approximately equal to the change in afterbody angle, which in turn is equal to twice the increase in static floating trim. These tendencies are confirmed at the lower loading in Figure 6 (b), the differences in weight seeming to have little effect. As in the displacement speed range buoyancy forces predominate, the trim changes are almost independent of elevator setting, but over the planing speed range they vary, the increase in trim due to a given increase in afterbody angle being, in general, greater for the lower values of elevator angle and greater at the higher speeds.

The effect of afterbody angle on amplitudes of porpoising is shown in both undisturbed and disturbed cases for one load ($C_{\Delta_o} = 2.75$) in Figure 7. In the undisturbed case it appears that there is little difference between the 4° and 8° afterbody angle models, but it should be noted that the data are rather sparse and, as the majority of the points for Model E (Figure 7 (c)) lie on the limits, they are, by definition, of 2° amplitude. The general level of porpoising amplitudes for the 6° afterbody angle model (Figure 7 (b)) does, however, seem to be slightly higher than the others. In the disturbed case, with the change in afterbody angle from 4° to 6°, there is a large increase in the amplitudes of porpoising, while a further change in angle from 6° to 8° produces a further, but very slight increase. Raising the afterbody angle has thus no significant effect on undisturbed porpoising amplitudes, while disturbed amplitudes show first a marked increase then a very slight increase. An examination of porpoising amplitudes at $C_{\Delta_o} = 2.25$ in References 3, 11 and 12 shows that weight change makes little difference and that the above conclusions are unaltered.

2. Previous investigations

There are many references to afterbody angle effects in various reports, but only three (References 13, 14 and 15) which treat the subject directly will be considered here. In each case, afterbody angle variations are considered as part of a much fuller investigation into the characteristics of low length beam ratio hulls and, as the three reports are American, the techniques used in the model tests differ from those used in the current programme. These differences have been considered in References 16 and 17, whence it appears that comparison should be made on the basis of steady speed runs; the N.A.C.A. lower limit and the upper limit, increasing trim than correspond to M.A.E.E. undisturbed limits, and the N.A.C.A. upper limit, decreasing trim corresponds to part of the M.A.E.E. limit with disturbance.

In Reference 13, the model used had a length/beam ratio of 6.3 and was tested at C_{Δ_0} = 0.87 (based on maximum beam). The forebody, which was 3.7 beams in length, had no warp, incorporated chine flare and had a main step deadrise of 20°. The depth of the main step was constant at 5.5% beam. A complete dynamic model was used in the tests, the mainplane being fitted with full span leading edge slats; no slipstream was used and the range of afterbody angles covered was from 5.3° to 9.8°. (The equivalent angles used in the figures of this reference are 4.0° and 8.5°; they are less than the angles just quoted by 1.3°, which is the angle of the forebody keel to the hull datum. As the hull datum is quite arbitrary in position it can have no influence on the hydrodynamic properties of the hull, so here and later, all afterbody angles quoted will conform to the definition given in the introduction, this being considered a better basis for comparison.)

The authors concluded that increasing the afterbody angle produced no marked changes in the position of the lower limit and a non-linear raising of the upper limit, which was greatest for the afterbody angle increment from 6.8° to 8.3°. The final increment, from 8.3° to 9.8°, was critical in that little increase in the stable trim range resulted and the character of the unstable motion was entirely changed with the higher afterbody angle, consisting mainly of vertical oscillations with little change in trim. It is then stated that for a given configuration there is an optimum afterbody angle and that too great an angle may even decrease the stable range of trims or lead to a more violent type of porpoising. Considering Figure 19 of this reference, which is a comparison of stability limits, and neglecting the 9.8° afterbody angle results for the minute, the nature of the other results is such that this figure would fit in well, about halfway (at say C_{Δ_0} = 2.5) between the two weight cases in Figures 2 and 3 of the present report. The post-hump separation of the lower limits (Figure 19, Reference 13) is $\frac{1}{2}$° and a slight tendency towards a neck of instability can be seen in the case of the 6.8° afterbody angle; there is also good correlation between the upper limits, decreasing trim and the present disturbed cases. If all the limits of Reference 13 are now considered, it appears that the optimum afterbody angle whose existence is suggested by the authors lies somewhere around 9°. If the existence of a similar critical afterbody angle be assumed in the present high length/beam ratio case, it would appear that it was either just reached or being approached, but had not been exceeded, with Model H (8° afterbody angle). Again, as afterbody angle effects are not independent of loading, this critical angle would probably vary with weight.

In the investigation of Reference 14, a hull of length/beam ratio 6.2 was tested at C_{Δ_0} = 0.89. The forebody was unwarped but had chine flare, a 20° main step deadrise angle and was 3.45 beams in length. The step depth was constant at 4.8% beam and the range of afterbody angles tested was from 2° to 12°. Dynamic hull models were used, aerodynamic moments and forces being fed in synthetically. It was concluded that increasing the afterbody angle raised the lower limit at moderate speeds and caused it to start at a slightly lower speed, but had no appreciable effect on the lower limit at high speeds; the upper limit was raised and, with the two greatest afterbody angles ($9\frac{1}{2}$° and 12°), the upper limit was suppressed at high speeds. Here there is no evidence of an optimum afterbody angle, in fact the changes are progressive and straightforward; but differences in the test techniques should be noted.

The tests of Reference 15 were made on models of four different length/beam ratios over a range of afterbody angles from 3° to 11° in each case. The basic hull form, from which the others were derived, had a length/beam ratio of 6.19 and a forebody length of 3.44 beams. It incorporated both forebody warp and chine flare and had a mainstep deadrise angle of 20° with a step depth of 5.0% beam. The conclusions, which are general and apply to each of the length/beam ratio cases, 5.07, 6.19, 7.32 and 8.45, state that the longitudinal

/ stability

stability limits are widened with increasing afterbody angle. Increasing afterbody angle raises the upper stability limits and causes the lower stability limits to occur at higher trims and at lower speeds. The author continues to say, in effect, that static and hump trims are raised, twice the increase in static floating trim being equal to the increase in hump trim, which in turn is equal to the increase in afterbody angle. It should be noted that the technique used in these tests was the same as that of the previous reference, i.e. aerodynamic forces and moments were applied synthetically.

The longitudinal stability limits are presented on a non-dimensional base and this may obscure any difference in the effects of increasing afterbody angle following a change in load. In the comparison of afterbody angle effects in Reference 15 (Page 44) the main trends are clear, but there are two interesting points of detail. The lower limits collapse at higher speeds, except in the case of the lowest length/beam ratio (5.07) models. Here the limits for the 3° afterbody angle show a vertical band of instability lying across the take-off path at high speeds. This band, occurring only with the 3° afterbody angle, is narrowed with increasing length/beam ratio and disappears with the models of length/beam ratio 7.32. All of the upper limits are raised progressively with increase in afterbody angle, except in the 7.32 length/beam ratio case, when that for the 11° afterbody angle crosses and runs below the 7° upper limit at the high speed end of the diagram.

2.3. Discussion

As the aim of this investigation is to provide design information, the variation of hull parameters has been kept within practical limits and the conclusions drawn will in general apply only within these limits. The range of afterbody angles tested thus deserves some comment.

The lowest afterbody angle (4°) is considered a reasonable minimum. At the design loading, $C_{\Delta_0} = 2.75$, undisturbed stability is acceptable but disturbed stability is bad, the deterioration with disturbance being marked; a further decrease in afterbody angle would worsen these qualities. With the highest afterbody angle (8°), on the other hand, good stability characteristics are obtained and had a higher angle still been tested it might have further improved these good qualities or, in the manner of Reference 13, it might not. It should be remembered, however, that one of the main objects in using a high length/beam ratio hull is to obtain low aerodynamic drag. It is known that the turn up of the hull camber line, obtained with contemporary afterbodies, can be responsible for a significant proportion of the hull drag[18], so a further increase in afterbody angle, which would in general produce a further increase in drag, is not considered necessary. It follows that, although increase in afterbody angle has been talked about (this is consistent with the reports on forebody warp and afterbody length, References 6 and 10) and this investigation indicates how variation of afterbody angle can improve longitudinal stability in the high length/beam ratio case, the immediate object is to find out by how much afterbody angle can be reduced, while maintaining reasonable stability characteristics.

In the undisturbed case the main effects on the longitudinal stability limits of increasing afterbody angle are to raise both the upper limit and maximum lower critical trim, thereby widening the available stable trim range. This general trend is found in all the cases which have been considered and is thus independent of length/beam ratio. In view of the discrepancies, however, between loads and between models, some detailed discussion is necessary.

/ Consider

Consider the lower limits obtained in the present investigation with the three different afterbody angles. At $C_{\Delta_0} = 2.75$ (Figure 2(a)) they are almost coincident; with a decrease in loading to $C_{\Delta_0} = 2.25$ they are lowered (Figure 3(a)), but the amount of this lowering for the 8° afterbody angle is only half of what it is for the 6° and 4° angles giving a separation of the limits at this weight. It is felt that this discrepancy can be accounted for mainly by the airflow under the afterbodies and the associated suctions and to a lesser extent perhaps, by the choice of the 2° double amplitude stability criterion. These points will be considered further at a later stage in the present investigation. It should be noted, however, that any suction effects which do occur will be emphasised in the present case, as the high beam loadings result in deeper troughs, the long afterbodies allow a greater moment arm and the two low afterbody angles tested are lower than those of contemporary afterbodies.[19] As a design factor, this additional displacement of the lower limit with weight, 1°, in the lowest afterbody angle case, could barely be ignored and any further change in the parameters which could increase or exaggerate afterbody suction effects, i.e. increase in afterbody length, change in design beam loading or further lowering of afterbody angle, should be cautiously applied to hulls of length/beam ratios of 10 or more. An immediate safeguard when considering high length/beam ratio designs with low afterbody angles would be to check stability at two or more weights during model tests. Any large reduction in the stable region resulting from a last minute increase in loading would not then be unexpected.

Considering now the upper limits without disturbance, the main conclusion in every case is that increasing afterbody angle raises the upper limit. In References 14 and 15, aerodynamic forces and moments were applied synthetically and, apart from one or two minor discrepancies in Reference 15, the results are straightforward. In Reference 13, where the representation of model aerodynamics was similar to that of the present investigation, it is suggested that there is an optimum afterbody angle of approximately 9° for the general configuration tested and above this the upper limit undisturbed is lowered. No inconsistencies were found in the present high length/beam ratio case, but the highest afterbody angle tested was only 8°. It is suggested that the reversal of the trend in Reference 13 with increasing afterbody angle is not an afterbody angle effect, but is a characteristic of the test technique. At the low Reynolds Numbers prevailing in tank tests, unslatted model tailplanes are inefficient and can be expected to commence stalling at relatively low incidences. This leads to aerodynamic static instability, which becomes important at high speeds and attitudes when the load on water is very small. With the highest afterbody angle in the present case, the load on water at a typical point on the upper limit ($C_{\Delta_0} = 2.75$, $C_V = 9.7$) is of the order of 1% of the model weight, when ground effect is considered. What the detailed effect of a further increase in attitude would be, would depend on the individual case, but as the load on water tends to zero the aerodynamic effects will be increasingly felt and results could become questionable.

In the disturbed case, there is a progressive improvement in stability with increase of afterbody angle, which is similar at both loadings. Each set of limits shows a vertical band of instability across the take-off path and this gets wider as the afterbody angle is lowered, until, with the 4° afterbody angle, it covers the greater part of the planing speed range. The low angle configuration as tested is, therefore, not a good design proposition, although this situation is somewhat mitigated by the facts that the amplitudes of disturbed porpoising are considerably less than those for the 6° and 8° afterbody angle models and, in the undisturbed case, there is effectively a clear stable take-off path at both loadings.

/ In

In a practical case, where good stability characteristics are the aim, the configuration with the highest afterbody angle would appear to be the best, but the hump attitude of 13.5° at C_{Δ_o} = 2.75, coupled possibly with a wing setting angle of about 2°, would, unless a wing of high aspect ratio were used, result in tip stalling and wing dropping. At the hump speed of C_V = 4.5 (V = 47 knots at 150,000 lb.) this could be dangerous. If, on the other hand, it was decided to use a low afterbody angle to obtain low air drag while maintaining acceptable hydrodynamic stability characteristics, the lowest angle tested could only be used under ideal operational conditions, i.e. conditions represented by the undisturbed limits. Alternatively, in order to use the lowest angle under normal operational conditions (apart from waves), when disturbed limits apply, some additional modification must be made to the hull form.

The present investigation into the effects of afterbody angle is a calm water one, with the undisturbed results representing the ideal case and the disturbed results covering normal operational hazards. No correlation has been found so far between wave and disturbance effects on stability over the whole of the planing speed range; further work is therefore necessary to determine the effects of afterbody angle on stability in waves.

3. WAKE FORMATION

The nature of the wake photographs for Models A, G and H does not allow an assessment of the wake depth or section and in this direction little is to be gleaned; what they do show, however, is whether or not the afterbody is touching the wake. In view of the discussion in the previous section this may be important, particularly in the case of the lowest afterbody angle. It can be seen that in the vicinity of the lower limit, the afterbody of Model G is in general clear of the wake, but there is a minor exception at C_{Δ_o} = 2.25; close to the point of maximum lower critical trim the aft step just touches the water. This, however, is at the low speed end of the planing range and may therefore have been expected. Results for Model A are similar, the aft step just touching the wake at the lower weight near the point of maximum critical trim, while the afterbody of Model H is at all times clear.

4. SPRAY

The spray characteristics of the models were evaluated during the undisturbed longitudinal stability runs with $\eta = -8°$, mainly over the displacement range of speeds, by taking three simultaneous photographs at each speed. The cameras used were positioned off the starboard bow, the starboard beam forward of the wing and the starboard beam aft of the wing. A chequered pattern, consisting of alternate black and white squares of quarter beam side, with the step point as origin, was painted on the starboard side of each model to aid in the analysis, which consisted of obtaining projections of the spray envelopes on the median plane only. In plotting the projections, velocity spray was included when it was integral with the main spray blister, this happening mainly at low displacement speeds; otherwise it was ignored. The profiles used were taken straight from the side view photographs and a limited parallax error was accepted; where this error tended to become large those parts of the photographs were not used. These projections are compared in Figure 8.

The effects of afterbody angle on spray are shown at the higher weight (C_{Δ_o} = 2.75) in Figure 8(a). In every case, the profile is discontinuous, indicating that the wing was struck by main spray; not one of these configurations therefore has good spray characteristics. As afterbody angle is increased, the low speed spray is improved, most of the improvement accruing from the first increment of angle (from 4° to 6°); at higher displacement speeds, corresponding to the profiles aft of the main step, the effect is reversed, the lowest blisters being obtained with the lowest afterbody angle, but, as at all times the tailplane and elevators were clear of spray, this is not significant. That there is an overall

/improvement

improvement in spray characteristics with increasing afterbody angle is confirmed at the lower weight, $C_{\Delta_0} = 2.25$, in Figure 8(b), but the effect is smaller at this weight. The general improvement due to the weight decrease is obvious in that the profiles are now continuous, showing that spray either cleared the model or barely touched the mainplane trailing edge.

The improvement in spray characteristics with increasing afterbody angle follows directly from the consequent increased attitudes at a given elevator setting. There will be minor changes in draught, but these should only have a small effect on spray. The movement backward of the spray origin, at a given speed, with the increase in attitude is small, but it can be seen when comparing the individual spray photographs; an example is given in Figure 9 at $C_V = 3.0$ approximately for $C_{\Delta_0} = 2.75$.

As in the best case (Model H) spray characteristics are only moderate, it follows that any similar high length/beam ratio design having a low afterbody angle must incorporate forebody warp[6] or some other modification to give good spray characteristics.

5. DIRECTIONAL STABILITY

For directional stability tests each model was towed from and pivoted at the C.G. so that it was free in pitch, yaw and heave, but constrained in roll. Steady speed runs were made over a range of speeds from 4 to 40 ft. per second and at each speed the model was yawed up to not more than 18°, moments to yaw the model being applied by means of strings attached to the wing tips level with the C.G. The direction and order of magnitude of the resulting hydrodynamic moment was judged by the operator through the pull in the strings, and the angle of yaw was read off a scale on the tailplane with an accuracy of about $\pm\frac{1}{2}^\circ$. The general form of the resulting stability diagram is considered in Reference 1, but it may be mentioned here that the model will swing towards a position of stable equilibrium and away from one of unstable equilibrium. The tests were made with no rudder trimming tab, and it was found that the effects of load[5], roll constraint[3] and elevator[3] on directional stability were small enough to be neglected. Stability diagrams for the models with afterbody angles of 4°, 6° and 8° are compared at one weight, $C_{\Delta_0} = 2.75$, in Figure 10.

The three diagrams are very similar, but with increasing afterbody angle an improvement in directional qualities is indicated; the low speed region bounded by the stable equilibrium lines and the 18° limit is widened in a direction parallel to the speed axis at values of yaw of about 5° and above, and the high speed unstable equilibrium line is moved out normal to the speed axis. These small changes would only have significance in a practical case at $C_V = 4$ roughly, when the flying boat was yawed past the unstable equilibrium line. With the 4° afterbody, at $C_V = 4$, this would occur at $\psi = 2^\circ$ and the yaw would automatically continue in the absence of corrective action to $\psi = 13^\circ$; with the 8° afterbody at this speed, the unstable equilibrium line would not be met till $\psi = 4^\circ$ and the yaw would be stopped at $\psi = 4\frac{1}{2}^\circ$. The 6° afterbody angle case lies between the 4° and 8° afterbody angle cases, but nearer to the 8°. Over the narrow speed band around $C_V = 4$ then, the improvement in directional stability with increasing afterbody angle is quite considerable; elsewhere it is negligible.

6. ELEVATOR EFFECTIVENESS

The effects of afterbody angle on mean elevator effectiveness are shown in Figure 11(a) for $C_{\Delta_0} = 2.75$. The curves obtained with the 6° and 8° afterbody angles show roughly the same values of effectiveness at a given speed, while values for the lowest afterbody angle (4°) are much lower.

/ With

With increasing afterbody angle then, it appears that elevator effectiveness increases rapidly at first and then remains almost unaltered. The same effects are shown in Figure 11(b) for $C_{\Delta_0} = 2.25$, the main difference between the two diagrams being the overall increase in effectiveness due to the decreased load.

The values of elevator effectiveness given in Figure 11 are mean values and a few remarks on them are necessary. Throughout this programme, when computing mean elevator effectiveness[1], the summation has been made from $\eta = -12^0$ to $+4^0$. On examining Figures 23, 27 and 23 of References 11, 3 and 12 respectively it can be seen that, while maximum values of effectiveness for Models A and G are well within this range, those for Model H lie near the $\eta = -12^0$ limit. It follows that had the summation for Model H been made over the range of say $\eta = -16^0$ to 0^0 higher mean values of elevator effectiveness would have been obtained for this model. This is not serious, however, and would make only a little difference to the conclusions drawn in the previous paragraph.

Reconsidering Figures 4(a) and 5(a), where the undisturbed stability limits are presented with elevator angles as ordinates in place of keel attitudes, it will be seen that while there is a movement of the limits with change of afterbody angle, there is no apparent, orderly improvement in stability. For a complete understanding of the results these figures should be considered in conjunction with the corresponding plots of elevator effectiveness.

7. CONCLUSIONS

The results of the present investigation show that the effects of increasing afterbody angle are

(i) to increase maximum lower critical trim and slightly reduce the speed at which it occurs,

(ii) to increase trim generally and, in particular, to increase hump trim and the maximum trim obtainable with normal elevators,

(iii) to raise the upper undisturbed stability limit considerably and, in general, to leave the lower limit unaltered,

(iv) to increase resistance to disturbance,

(v) to increase disturbed amplitudes of porpoising when the datum afterbody angle is low,

(vi) to move the spray origin backwards, giving rise to slightly improved spray characteristics (associated with (ii)),

(vii) to improve directional qualities over a narrow speed band just below hump speed,

(viii) to increase elevator effectiveness when, as in (v), the datum afterbody angle is low, and

(ix) to reduce slightly the elevator setting at which undisturbed, lower limit instability is encountered.

/ The

The afterbody angle effects listed above show, that if good stability characteristics are the prime consideration, the configuration with the highest afterbody angle is the best. Results (i) to (iii) are substantiated generally by References 13, 14 and 15 and may be said to be independent of length/beam ratio if only the tendencies and not the magnitudes of change are considered. An important detail of the high length/beam ratio stability case is that increase in afterbody angle causes the rate of change of lower critical trim with respect to load at constant speed[4] to decrease i.e. afterbody angle effects on stability are not independent of load; this applies to both undisturbed and disturbed cases. Whether, in a given case, there are two rates of change of critical trim with load, one for above and one below a certain critical afterbody angle, both of which will probably vary with length/beam ratio, or whether there is a critical angle which is purely a function of the beam loading, are points which, it is felt, are probably worth further investigation. Tests at two loads, however, would remove any doubts about the rate of change of lower critical trim with respect to load being too high and should be made in any case where it is thought that some secondary effect may be present e.g. on high length/beam ratio hulls having low, unventilated afterbodies.

This investigation is a calm water one with representative tests for operational conditions, i.e. disturbance tests. No satisfactory correlation, however, has yet been established between disturbance and wave effects on hydrodynamic longitudinal stability over the whole of the planing speed range; further work is therefore proposed to determine the effects of afte body angle in waves and to correlate them, if possible, with the effects of disturbance.

/ LIST OF SYMBOLS

LIST OF SYMBOLS

b	beam of model
C_L	lift coefficient = $L/\frac{1}{2}\rho SV^2$ (L = lift, ρ = air density)
C_V	velocity coefficient = $V/\sqrt{gb}$
C_Δ	load coefficient = Δ/wb^3 (Δ = load on water and w = weight per unit volume of water)
C_{Δ_c}	load coefficient at $V = 0$
C_X	longitudinal spray coefficient = x/b
C_Y	lateral spray coefficient = y/b
C_Z	vertical spray coefficient = z/b
	{(x,y,z) co-ordinates of points on spray envelope relative to axes through step point}
S	gross wing area
V	velocity
α_K	keel attitude
η	elevator setting
ψ	angle of yaw

/ LIST OF REFERENCES

LIST OF REFERENCES

Ref. No.	Author(s)	Title
1	D.M. Ridland J.K. Friswell A.G. Kurn	Investigation of High Length/beam Ratio Seaplane Hulls with High Beam Loadings: Hydrodynamic Stability Part 1: Techniques and Presentation of Results of Model Tests. Current Paper No. 201. September 1953.
2	J.K. Friswell A.G. Kurn D.M. Ridland	Investigation of High Length/Beam Ratio Seaplane Hulls with High Beam Loadings: Hydrodynamic Stability Part 2: The Effect of Changes in the Mass, Moment of Inertia and Radius of Gyration on Longitudinal Stability Limits. Current Paper No. 202. September 1953.
3	D.M. Ridland J.K. Friswell A.G. Kurn	Investigation of High Length/Beam Ratio Seaplane Hulls with High Beam Loadings: Hydrodynamic Stability Part 3: The Stability and Spray Characteristics of Model A. M.A.E.E. Report F/Res/237. February 1954. A.R.C. 16,627.
4	D.M. Ridland A.G. Kurn J.K. Friswell	Investigation of High Length/Beam Ratio Seaplane Hulls with High Beam Loadings: Hydrodynamic Stability Part 4: The Stability and Spray Characteristics of Model B. M.A.E.E. Report F/Res/238. March 1954. A.R.C. 16,761.
5	J.K. Friswell D.M. Ridland A.G. Kurn	Investigation of High Length/Beam Ratio Seaplane Hulls with High Beam Loadings: Hydrodynamic Stability Part 5: The Stability and Spray Characteristics of Model C. M.A.E.E. Report F/Res/239. October 1953. A.R.C. 16,762.
6	D.M. Ridland	Investigation of High Length/Beam Ratio Seaplane Hulls with High Beam Loadings: Hydrodynamic Stability Part 6: The Effect of Forebody Warp on Stability and Spray Characteristics. Current Paper No. 203. May 1954.
7	J.K. Friswell	Investigation of High Length/Beam Ratio Seaplane Hulls with High Beam Loadings: Hydrodynamic Stability Part 7: The Stability and Spray Characteristics of Model D. M.A.E.E. Report F/Res/241. November 1953. A.R.C. 16,753.
8	D.M. Ridland	Investigation of High Length/Beam Ratio Seaplane Hulls with High Beam Loadings: Hydrodynamic Stability Part 8: The Stability and Spray Characteristics of Model E. M.A.E.E. Report F/Res/242. December 1953. A.R.C. 16,791.
9	A.G. Kurn	Investigation of High Length/Beam Ratio Seaplane Hulls with High Beam Loadings: Hydrodynamic Stability Part 9: The Stability and Spray Characteristics of Model F. M.A.E.E. Report F/Res/243. February 1954. A.R.C. 17,034.

/ 10.

LIST OF REFERENCES (CONTD.)

Ref. No	Author(s)	Title
10	D.M. Ridland	Investigation of High Length/Beam Ratio Seaplane Hulls with High Beam Loadings: Hydrodynamic Stability Part 10: The Effect of Afterbody Length on Stability and Spray Characteristics. Current Paper No. 204. [illegible] August 1954.
11	D.M. Ridland A.G. Kurn J.K. Friswell	Investigation of High Length/Beam Ratio Seaplane Hulls with High Beam Loadings: Hydrodynamic Stability Part 11: The Stability and Spray Characteristics of Model G. M.A.E.E. Report F/Res/246. April 1954. A.R.C. 17,360.
12	J.K. Friswell D.M. Ridland A.G. Kurn	Investigation of High Length/Beam Ratio Seaplane Hulls with High Beam Loadings: Hydrodynamic Stability Part 12: The Stability and Spray Characteristics of Model H. M.A.E.E. Report F/Res/247. February 1954. A.R.C. 16,964.
13	N.S. Land L.J. Lina	Tests of a Dynamic Model in N.A.C.A. Tank No.1 to determine the effect of Length of Afterbody, Angle of Afterbody Keel, Gross Load, and a Pointed Step on Landing and Planing stability. NACA ARR. WR-L-400 (U.S.A.) March 1943.
14	K.S.M. Davidson F.W.S. Locke	Some Systematic Model Experiments on the Porposing Characteristics of Flying Boat Hulls. NACA. ARR. 3F12 (U.S.A.) June 1943.
15	A. Strumpf	Model Tests on a Standard Series of Flying-boat Hulls. Stevens Institute of Technology E.T.T. Report No. 325 (U.S.A.) May 1947.
16	A.G. Smith H.G. White	A Review of Porpoising Instability of Seaplanes. ARC. R & M 2852. February 1944.
17	J.P. Gott	Note on the Comparison of British and American Methods of Tank Testing Dynamic Models of Flying-boats. R.A.E. TN. Aero 1197 May 1943. A.R.C. 6892.
18	A.G. Smith J.E. Allen	Water and Air Performance of Seaplane Hulls as Affected by Fairing and Fineness Ratio. ARC. R & M 2896. August 1950.
19	A.G. Smith J.A. Hamilton	Notes on a Detailed Research Programme on Aero and Hydrodynamics of Hulls with High Fineness Ratio and Full Step Fairings. M.A.E.E. Report F/Res/221. March 1951. A.R.C. 13,877.

/ TABLE I

TABLE I

Models for hydrodynamic stability tests

Model	Forebody warp	Afterbody length	Afterbody-forebody keel angle	Step form	To determine effect of
	degrees per beam	beams	degrees		
A	0	5	6	Unfaired transverse. Step depth 0.15 beam.	Forebody warp
B	4	5	6		
C	8	5	6		
D	0	4	6		Afterbody length
A	0	5	6		
E	0	7	6		
F	0	9	6		
G	0	5	4		Afterbody angle
A	0	5	6		
H	0	5	8		
A	0	5	6		Tailored afterbody
J	0	5	6		
A	0	5	6		Interaction of parameters
B	4	5	6		
E	0	7	6		
H	0	5	8		
K	4	5	8		
L	4	7	6		
M	0	7	8		
N	4	7	8		

/ TABLE II

TABLE II

MODEL HYDRODYNAMIC DATA

Beam at step (b)	0.475'		
Length of forebody (6b)	2.850'		
Length of afterbody (5b)	2.375'		
Forebody deadrise at step	25°		
Forebody warp (per beam)	0°		
Afterbody deadrise	30° (decreasing to 26° at main step over forward 40% of afterbody length).		
Model	G	A	H
Afterbody angle	4°	6°	8°
Pitching moment of inertia (lb. ft.^{2})			
at C_{Δ_o} = 2.75	23.50	22.90	23.50
at C_{Δ_o} = 2.25	23.50	24.46	23.50

/ TABLE III

TABLE III

Model Aerodynamic Data

Mainplane		
Section		Gottingen 436 (mod.)
Gross area		6.85 sq. ft.
Span		6.27 ft.
S.M.C.		1.09 ft.
Aspect ratio		5.75
Dihedral	on 30% spar axis	3° 0'
Sweepback	on 30% spar axis	4° 0'
Wing setting (root chord to hull datum)		6° 9'
Tailplane		
Section		R.A.F. 30 (mod.)
Gross area		1.33 sq. ft.
Span		2.16 ft.
Total elevator area		0.72 sq. ft.
Tailplane setting (root chord to hull datum)		2° 0'
Fin		
Section		R.A.F. 30
Gross area		0.80 sq. ft.
Height		1.14 ft.
General		
* C.G. position		
distance forward of step point		0.237 ft.
distance above step point		0.731 ft.
* ¼ chord point S.M.C.		
distance forward of step point		0.277 ft.
distance above step point		1.015 ft.
* Tail arm (C.G. to hinge axis)		3.1 ft.
* Height of tailplane root chord L.E. above hull crown		0.72 ft.

*These distances are measured either parallel to or normal to the hull datum.

FIG 1

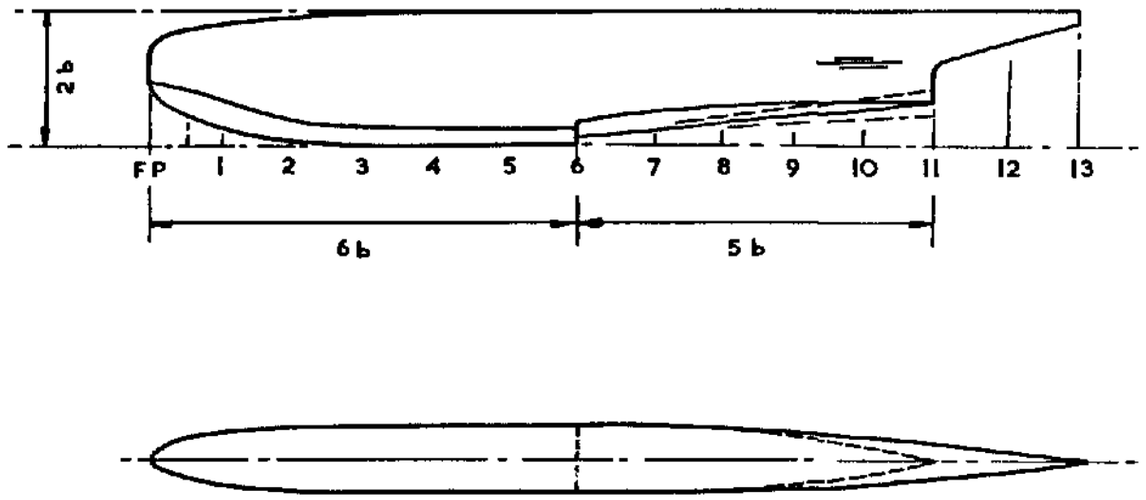

HALF MODEL SCALE

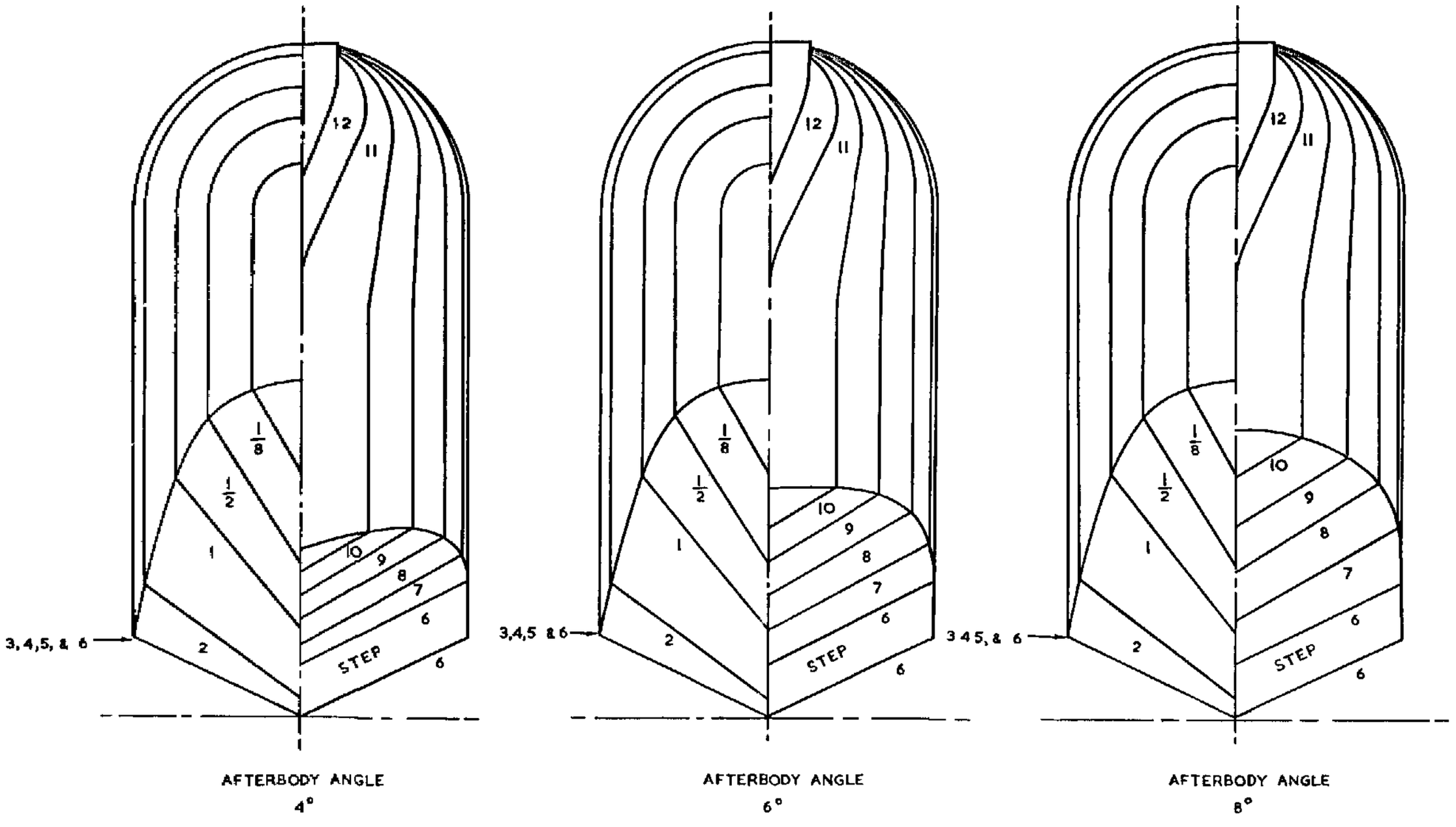

COMPARISON OF HULL LINES

FIG. 2.

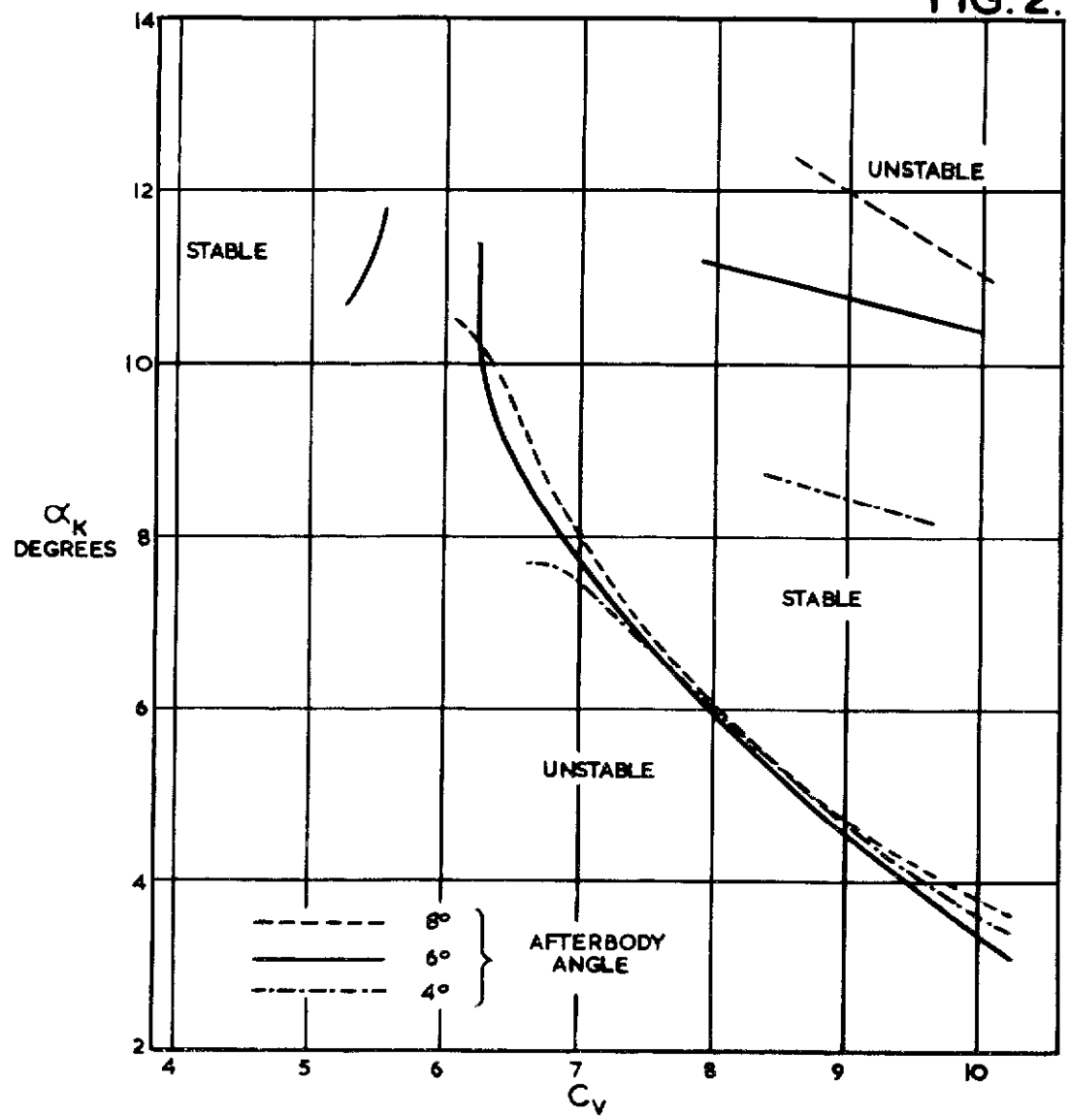

(a) UNDISTURBED

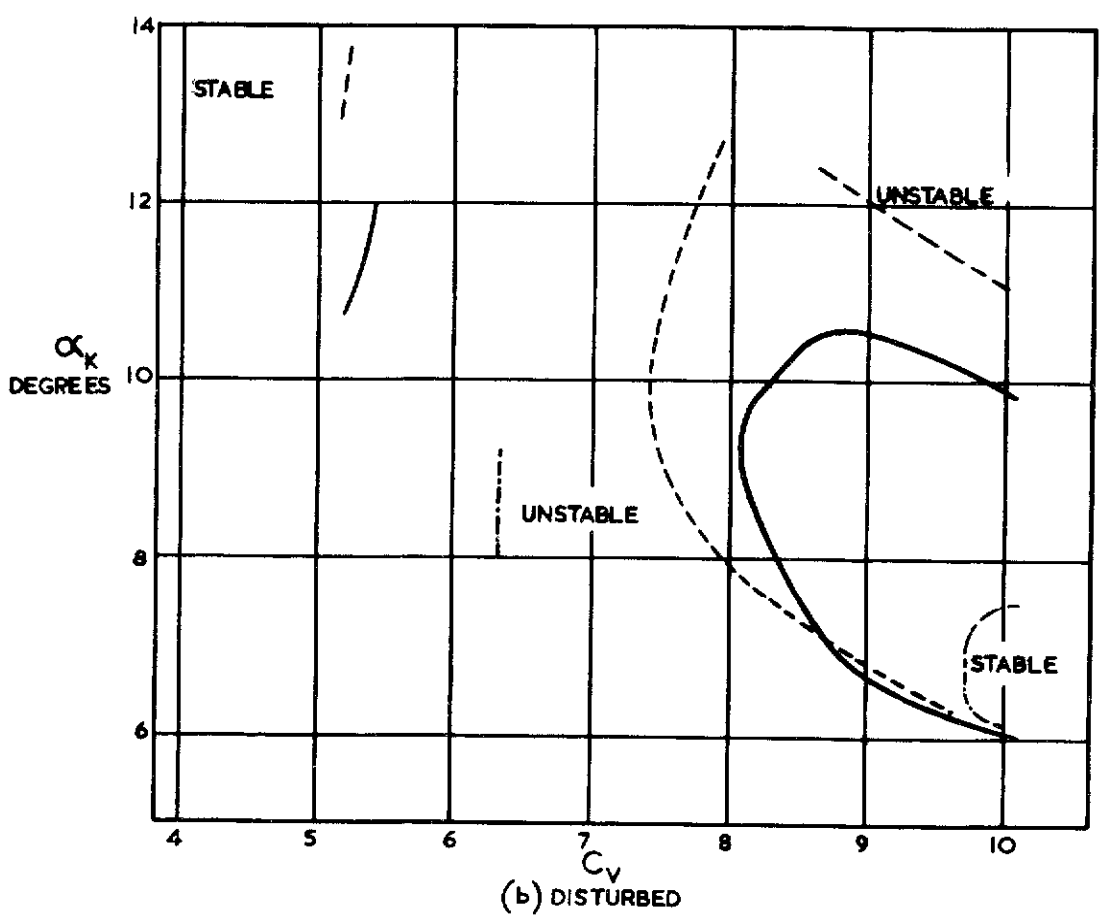

(b) DISTURBED

EFFECT OF AFTERBODY ANGLE ON LONGITUDINAL STABILITY LIMITS, $C_{\Delta_o} = 2{\cdot}75$.

FIG.3.

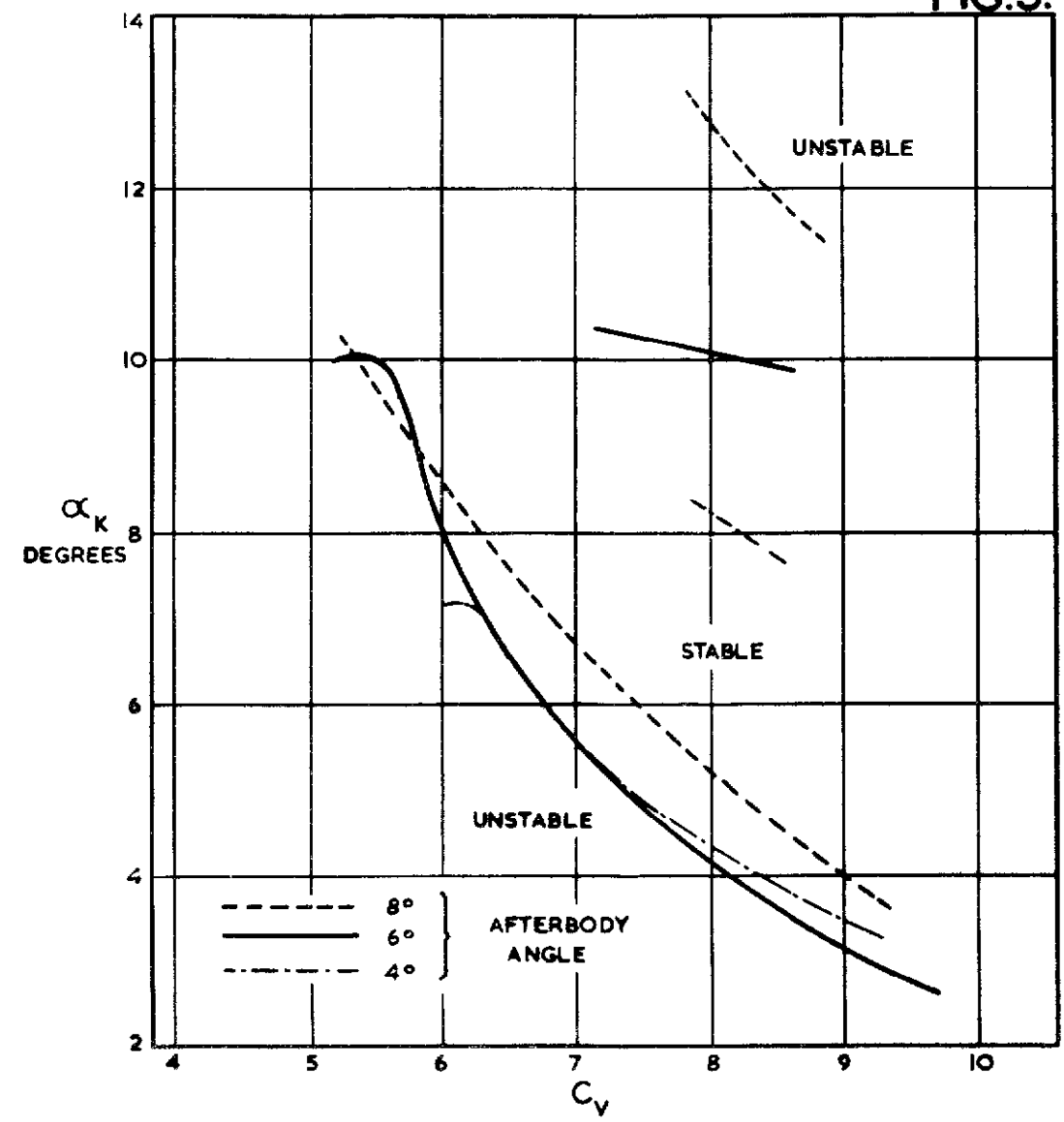

(a) UNDISTURBED

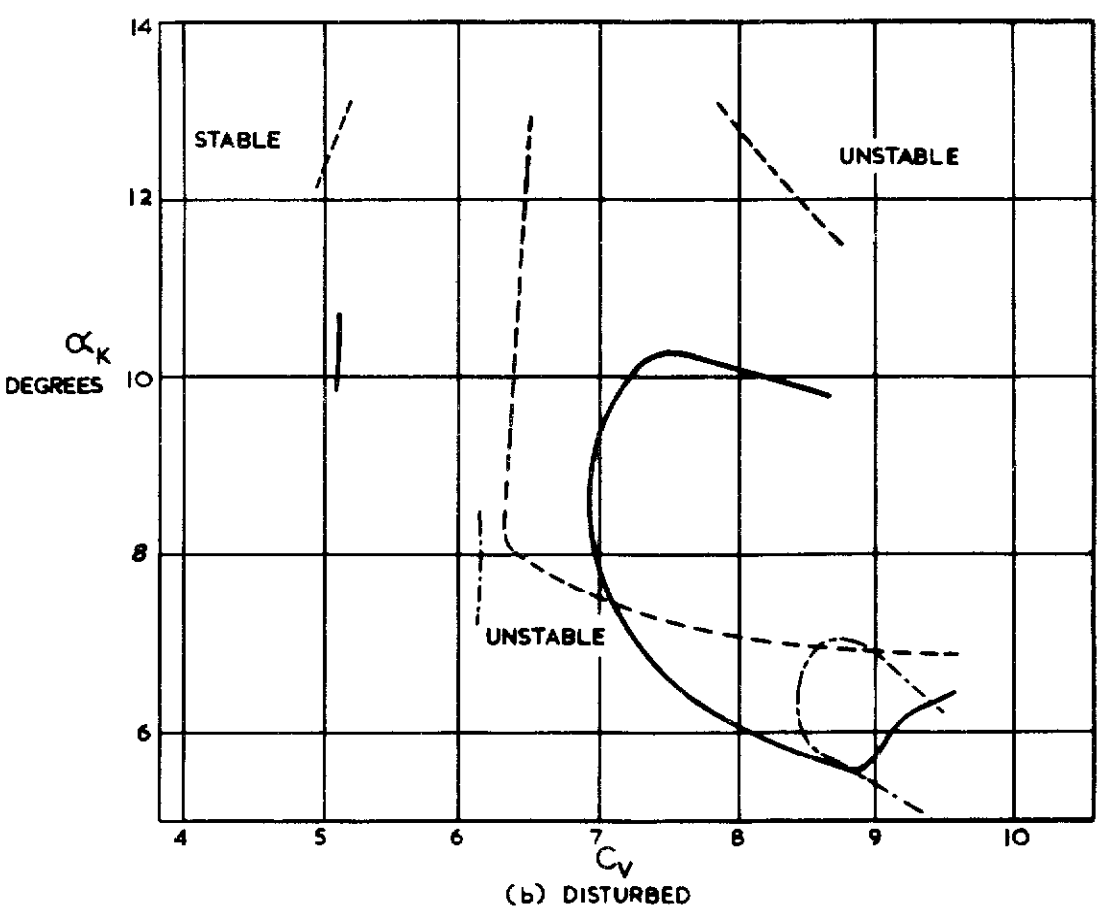

(b) DISTURBED

EFFECT OF AFTERBODY ANGLE ON LONGITUDINAL STABILITY LIMITS, C_{A_o} = 2·25.

FIG. 4.

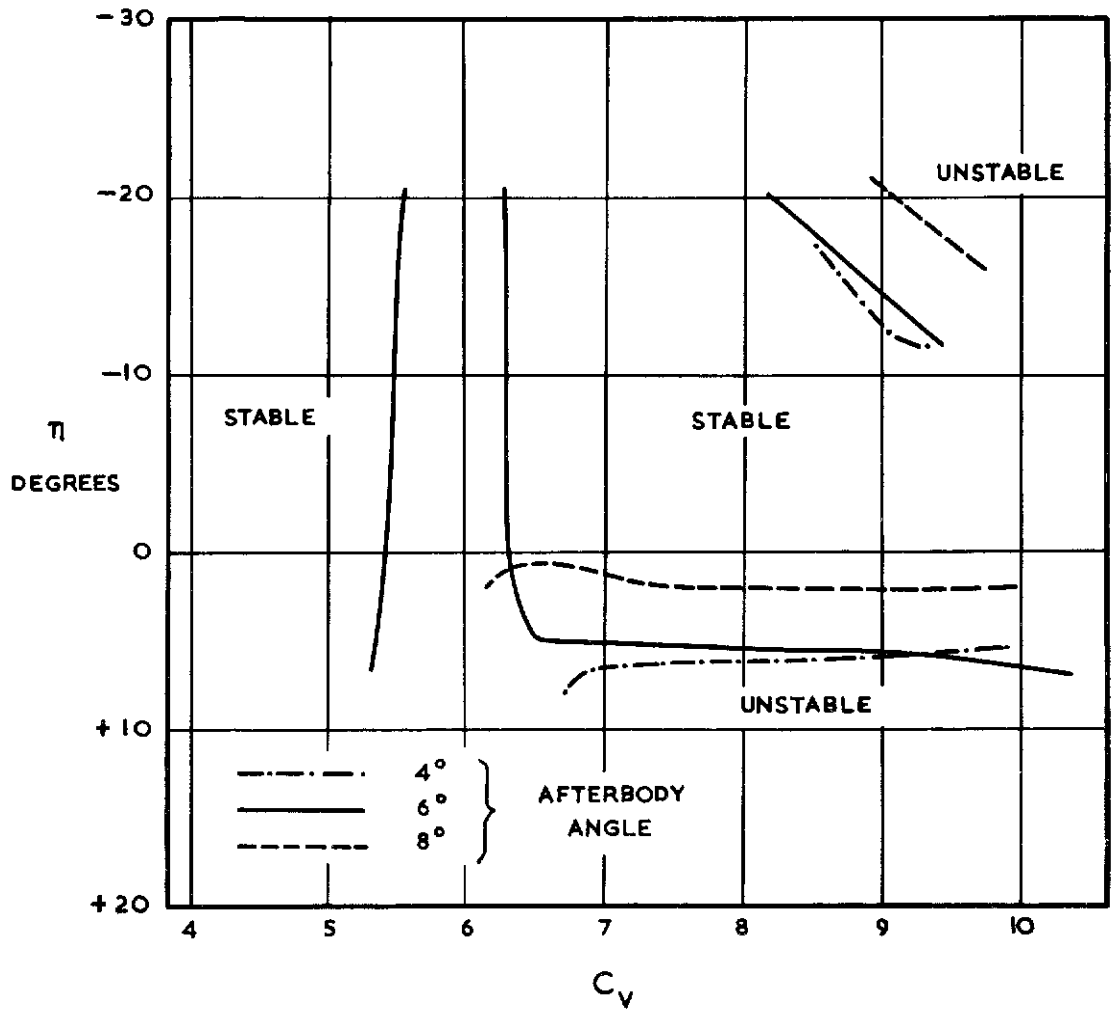

(a) UNDISTURBED

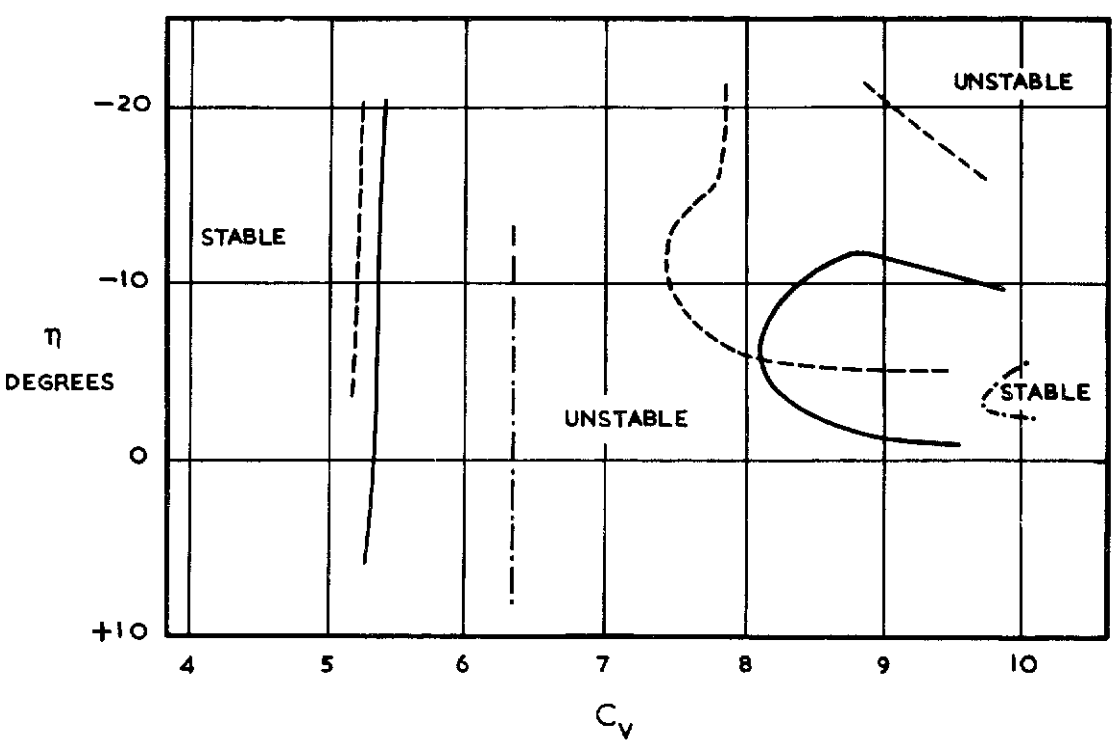

(b) DISTURBED

RELATION BETWEEN ELEVATOR SETTING AND STABILITY LIMITS
$C_{\Delta_o} = 2{\cdot}75$

FIG. 5.

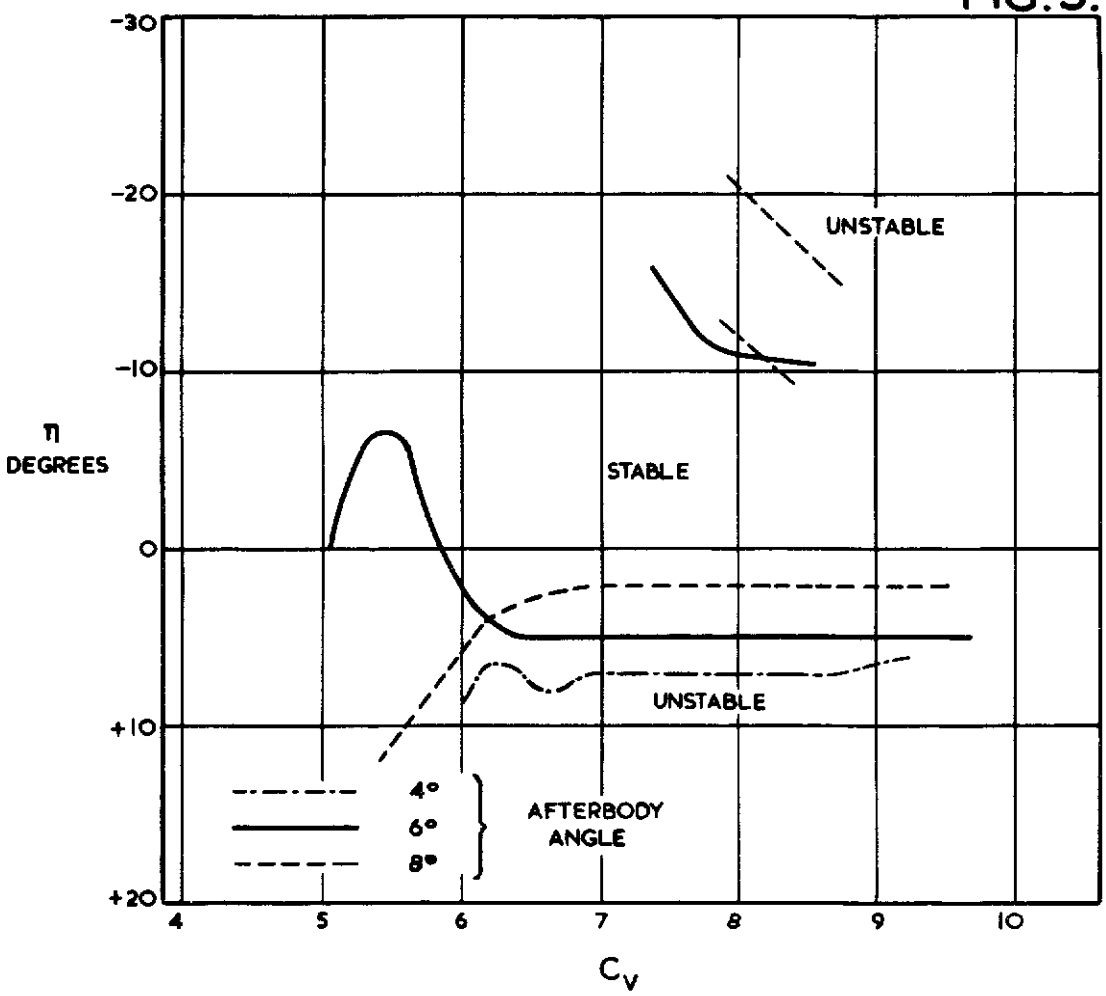

(a) UNDISTURBED

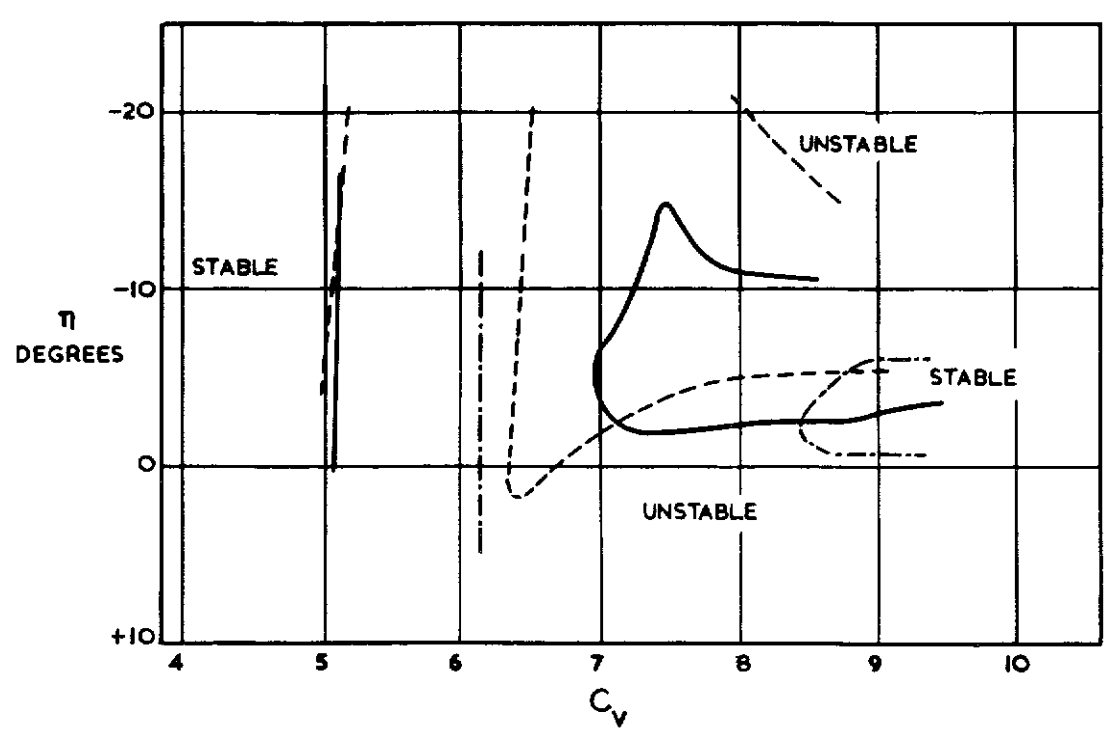

(b) DISTURBED

RELATION BETWEEN ELEVATOR SETTING AND STABILITY LIMITS
$C_{\Delta_o} = 2{\cdot}25$

FIG. 6.

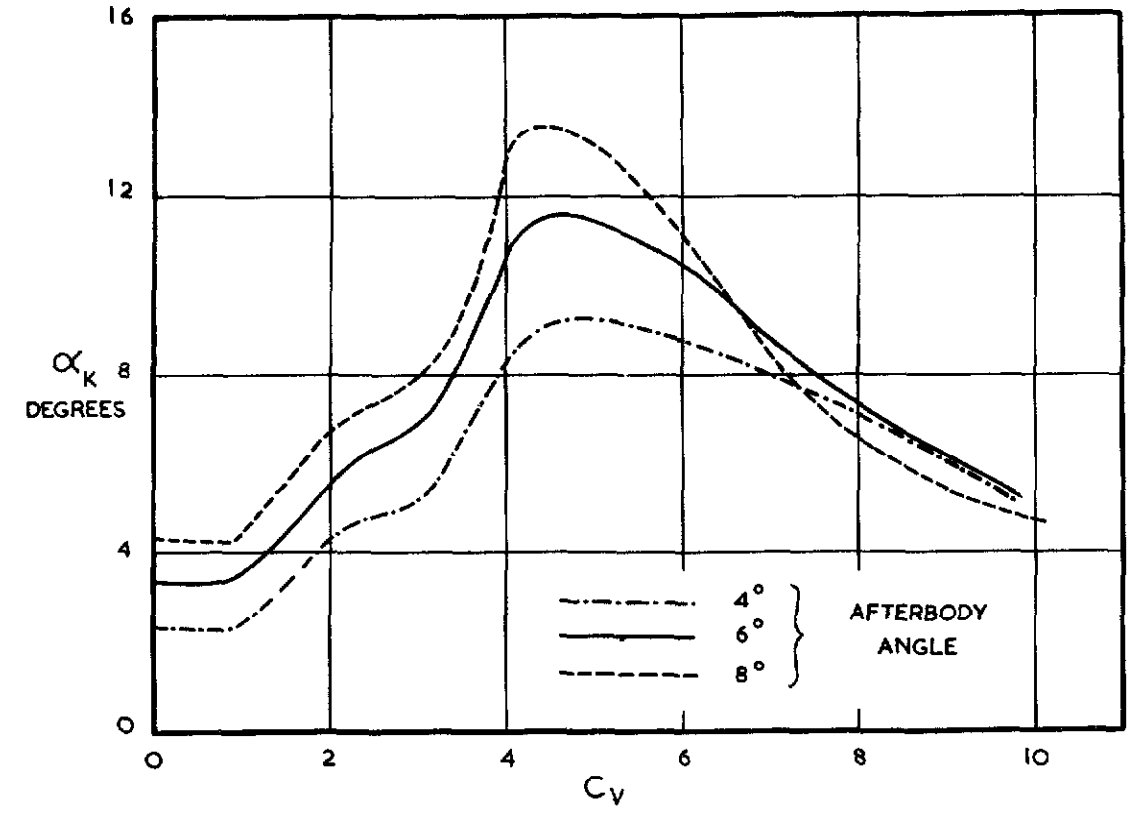

(a) $C_{\Delta_o} = 2{\cdot}75$

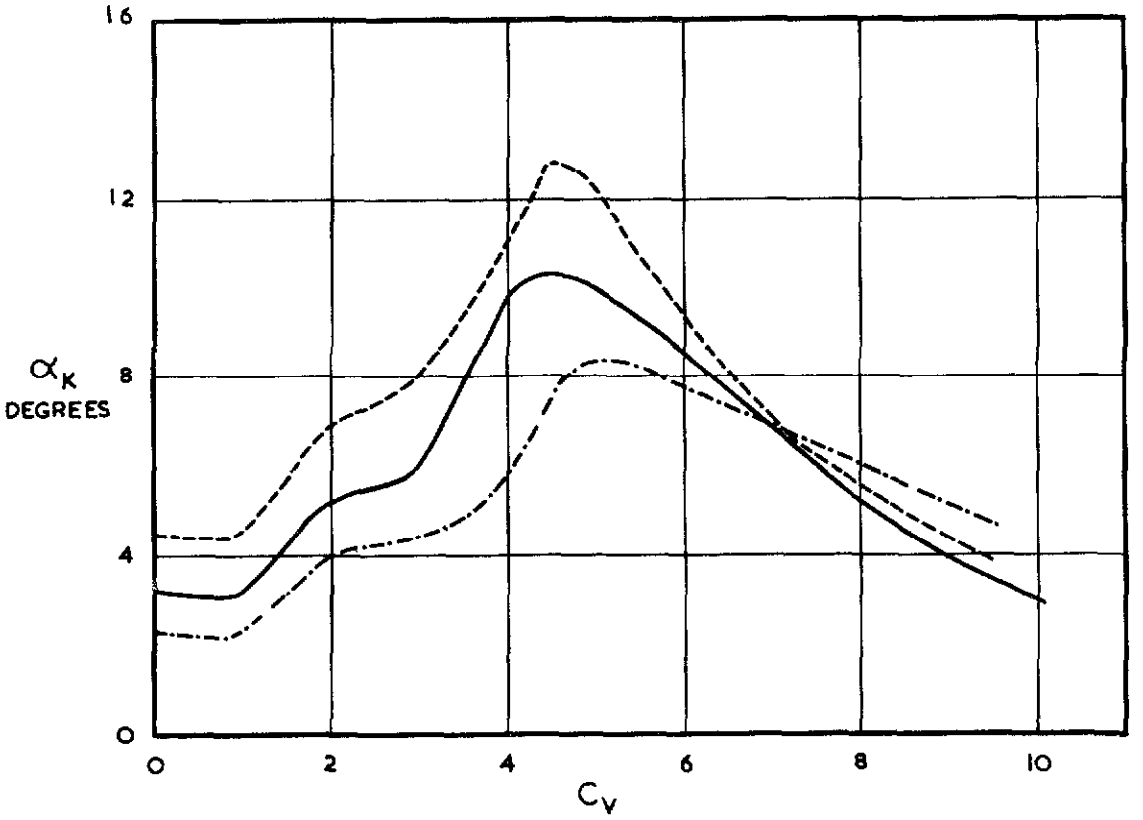

(b) $C_{\Delta_o} = 2\ 25$

EFFECT OF AFTERBODY ANGLE ON TRIM CURVES, $\eta = 0°$

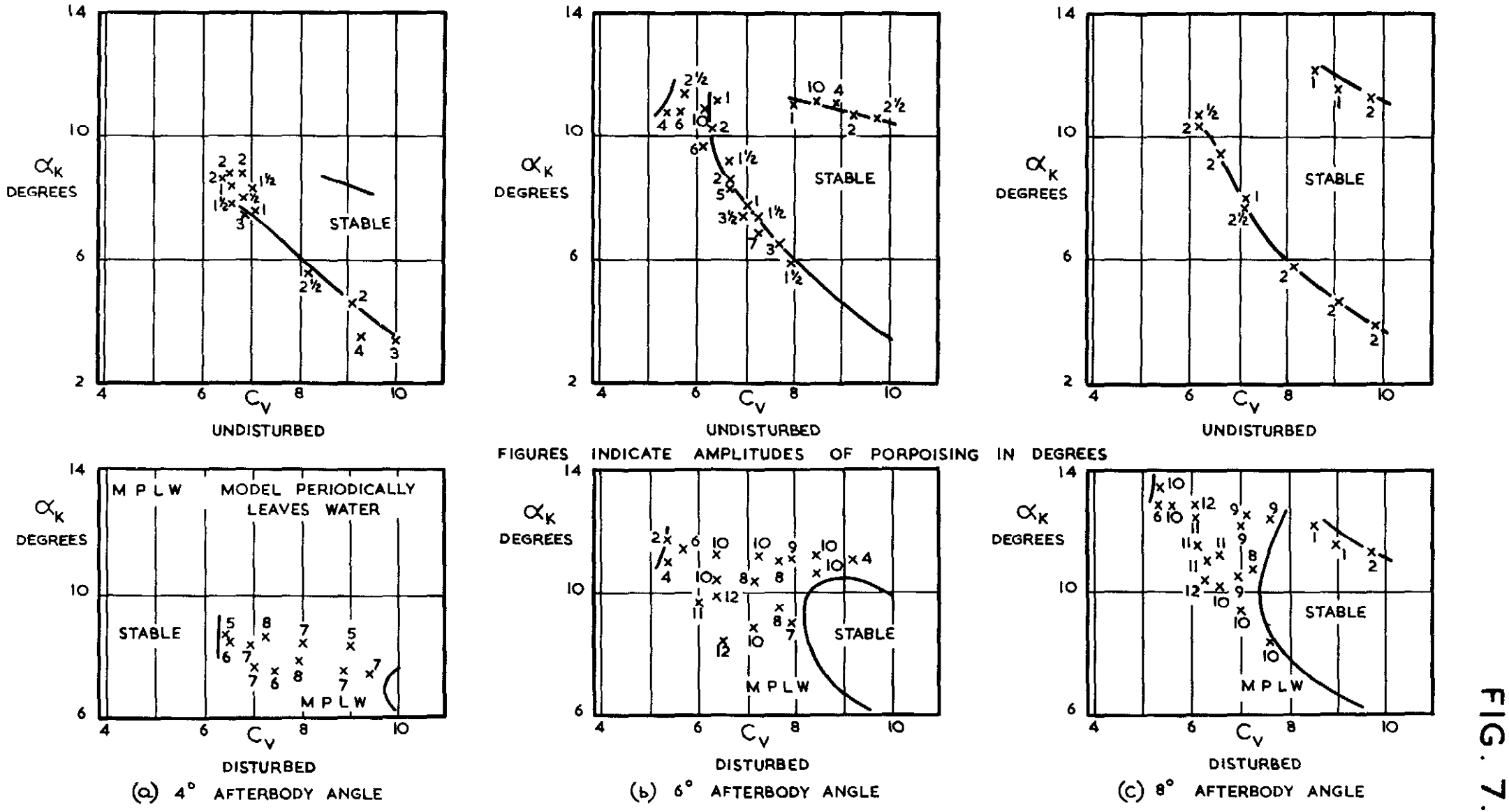

FIG. 7.

EFFECT OF AFTERBODY ANGLE ON AMPLITUDES OF PORPOISING, $C_{\Delta_0} = 2.75$

FIG. 8.

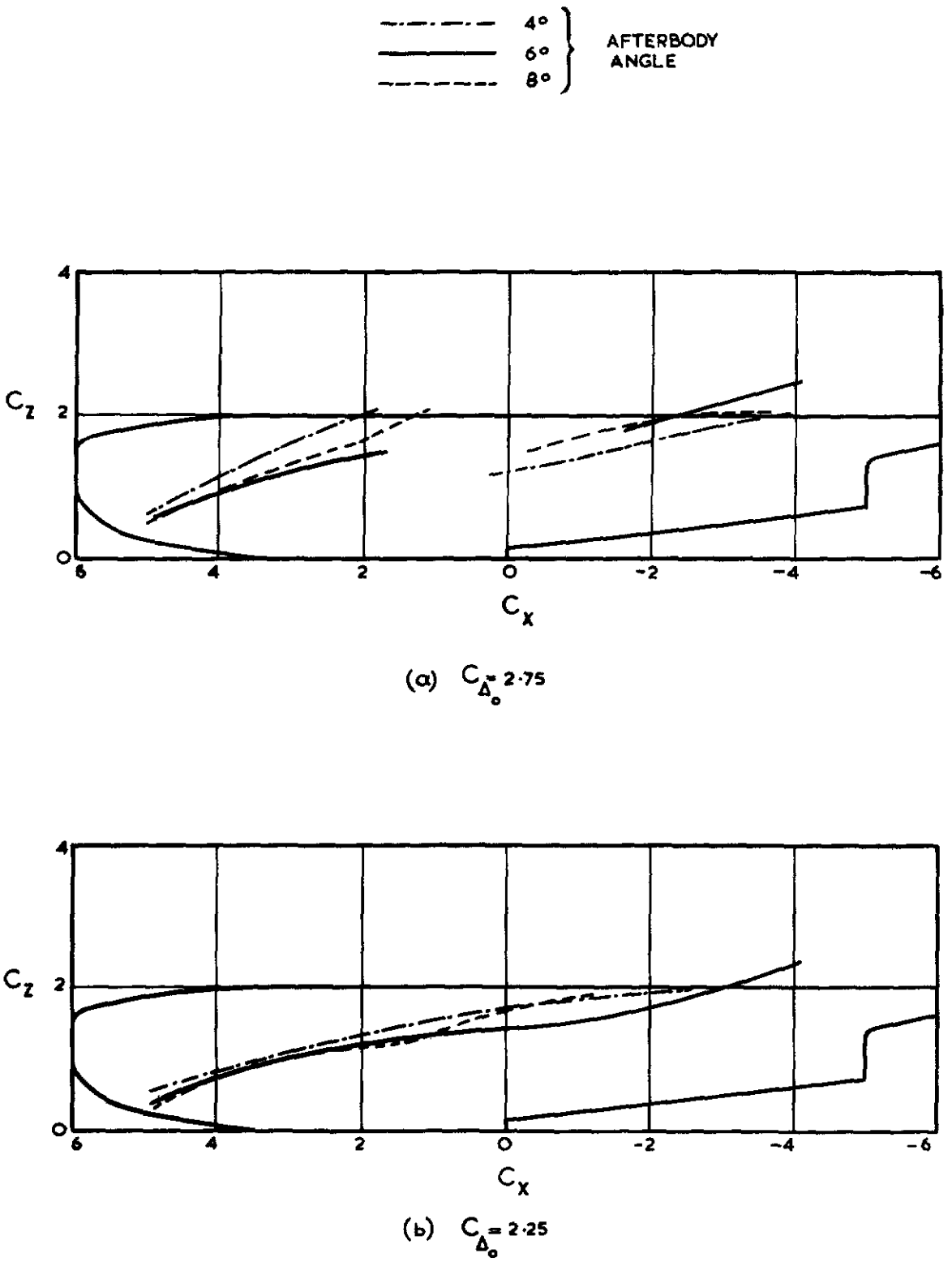

EFFECT OF AFTERBODY ANGLE ON SPRAY PROJECTIONS

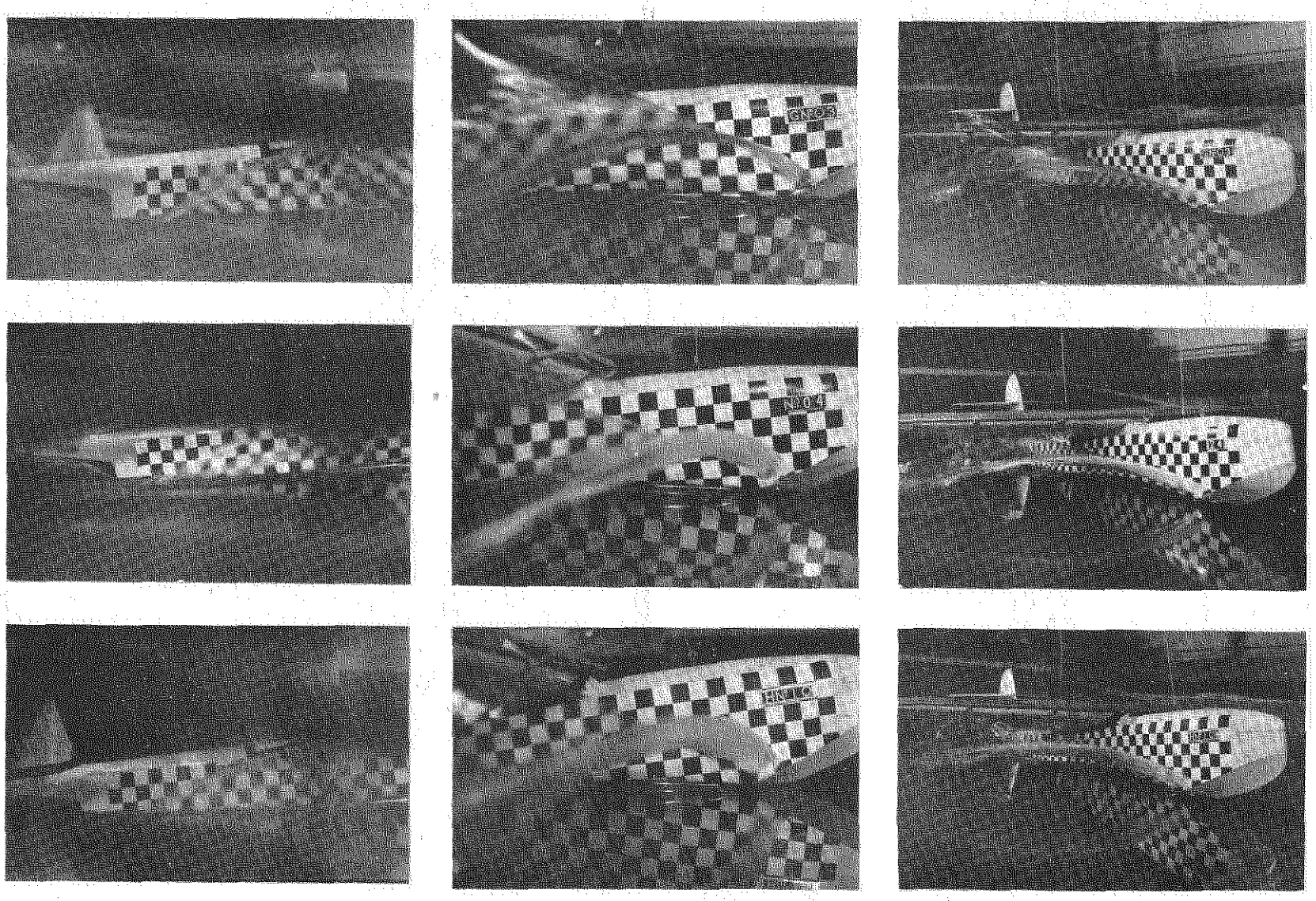

EFFECT OF AFTERBODY ANGLE ON SPRAY, C_{L_0} = 2·75

FIG.9.

FIG. 10.

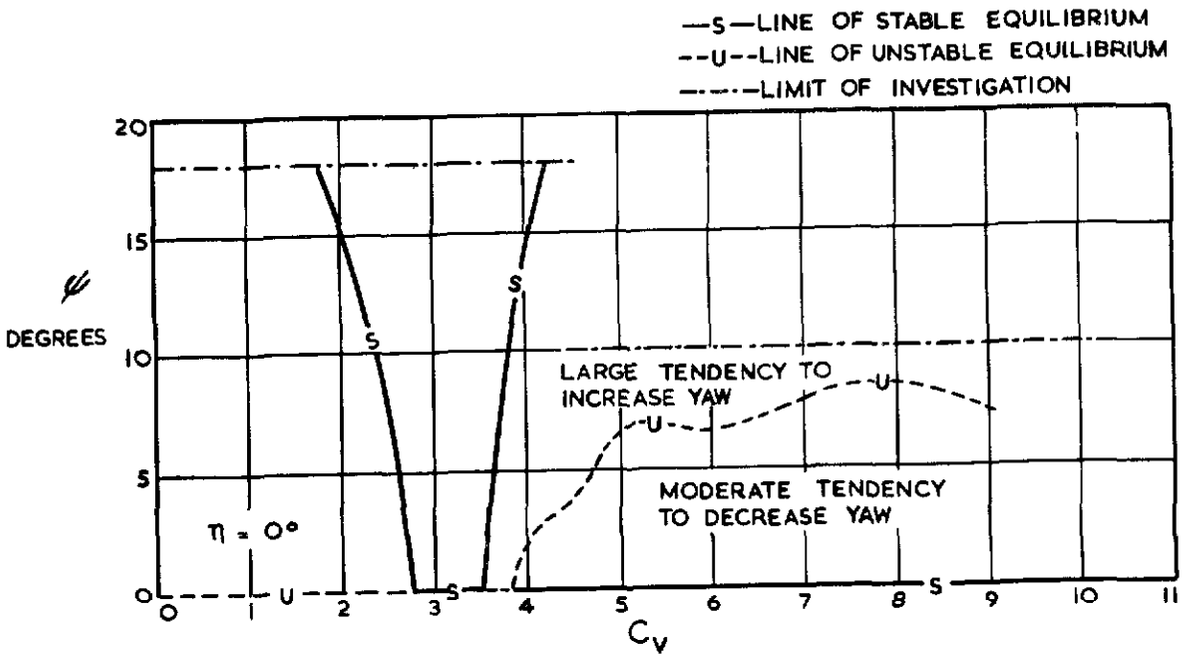

(a) 4° AFTERBODY ANGLE

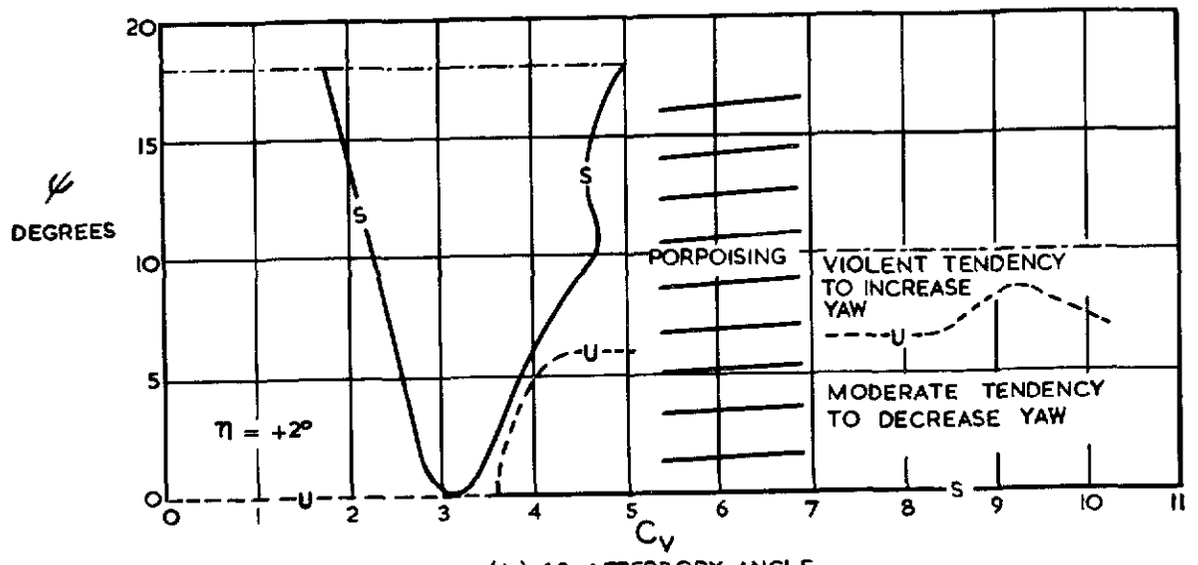

(b) 6° AFTERBODY ANGLE

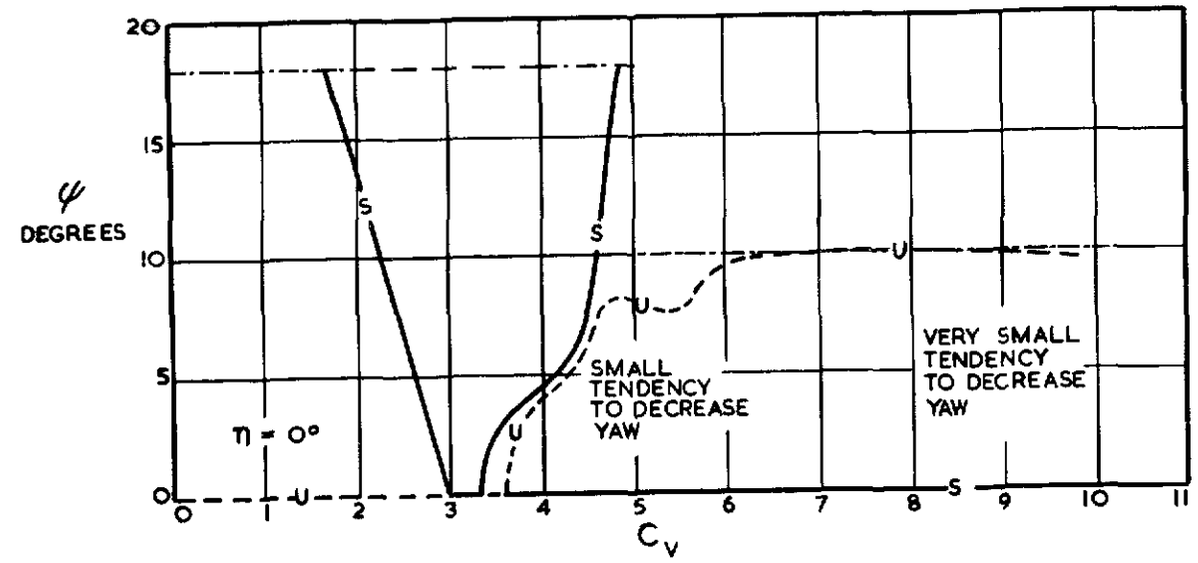

(c) 8° AFTERBODY ANGLE

EFFECT OF AFTERBODY ANGLE ON DIRECTIONAL STABILITY, $C_{\Delta_o} = 2.75$.

FIG. 11.

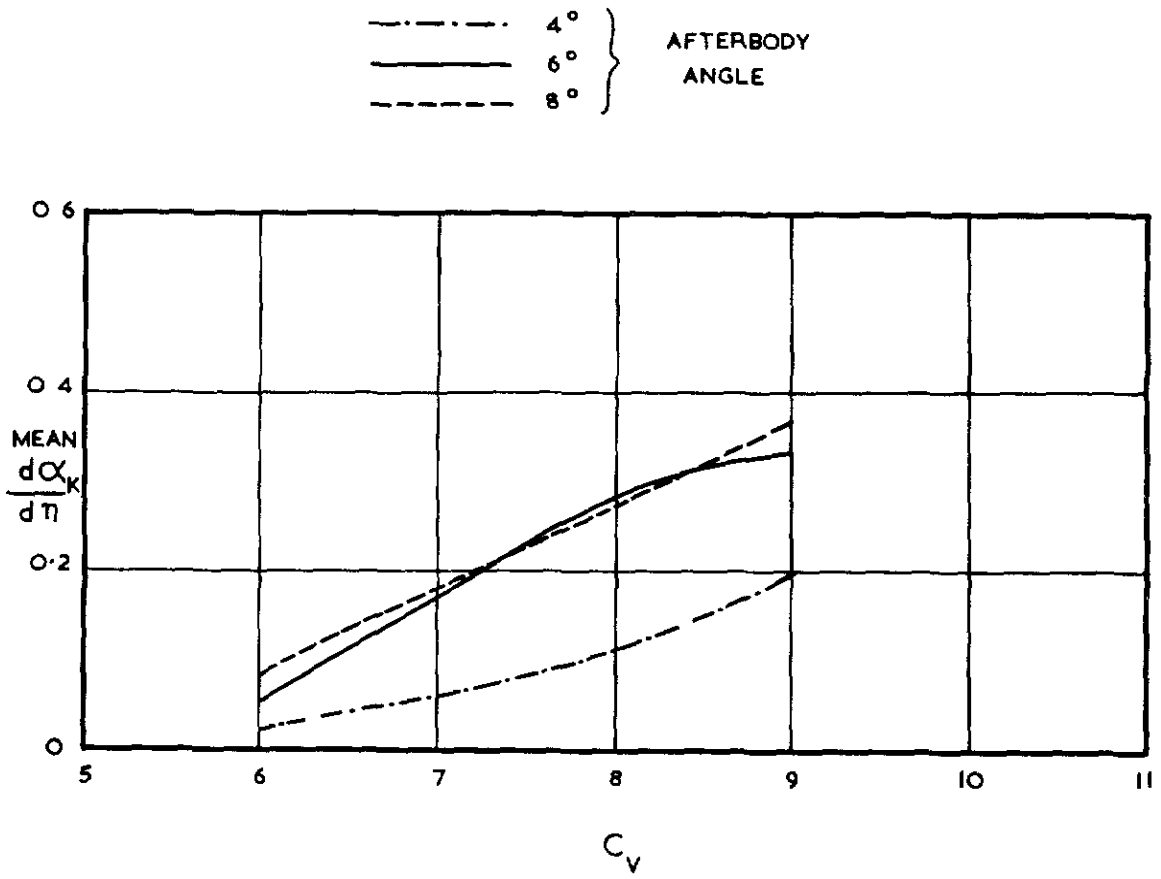

(a) $C_{\Delta_0} = 2.75$

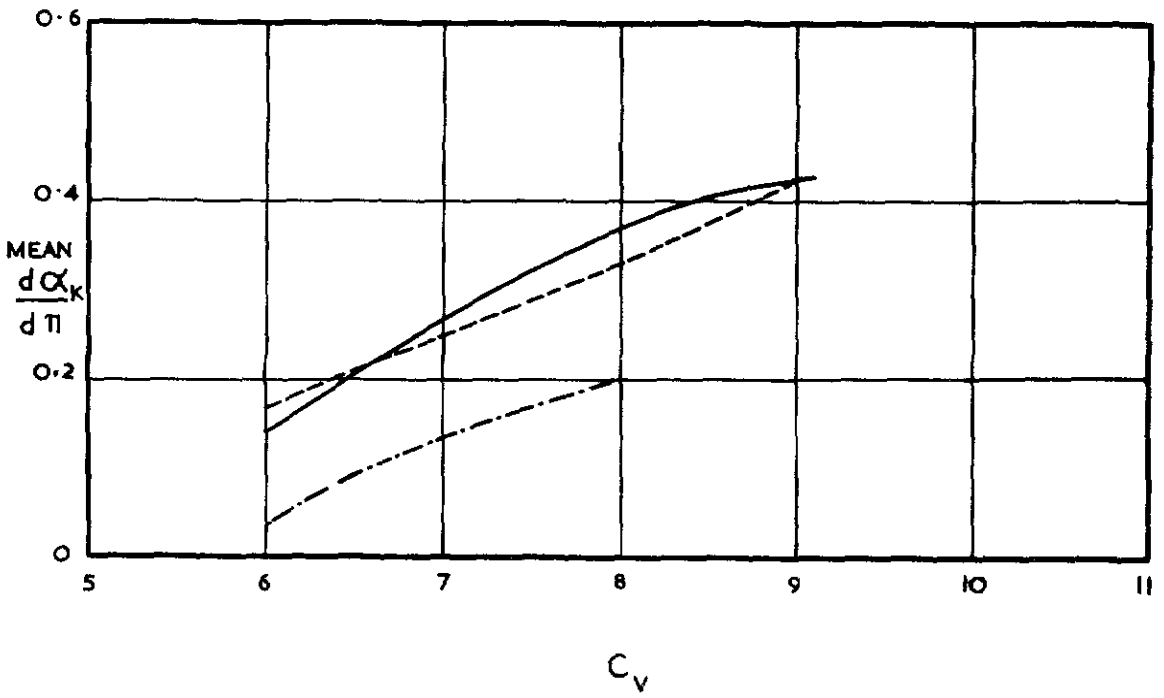

(b) $C_{\Delta_0} = 2.25$

EFFECT OF AFTERBODY ANGLE ON ELEVATOR EFFECTIVENESS

C.P. No. 236
(17,893)
A.R.C. Technical Report

Printed and published by
HER MAJESTY'S STATIONERY OFFICE

To be purchased from
York House, Kingsway, London W.C.2
423 Oxford Street, London W.1
P.O. Box 569, London S.E.1
13A Castle Street, Edinburgh 2
109 St. Mary Street, Cardiff
39 King Street, Manchester 2
Tower Lane, Bristol 1
2 Edmund Street, Birmingham 3
80 Chichester Street, Belfast
or through any bookseller

Printed in Great Britain

S.O. Code No. 23-9009-36

C.P. No. 236